Fibers and Polymers 2015, Vol.16, No.4, 782-787
DOI 10.1007/s12221-015-0782-6

ISSN 1229-9197 (print version)
ISSN 1875-0052 (electronic version)

EGF-loaded Nanofibrous Scaffold for Skin Tissue Engineering Applications

Mohammad Norouzi, Iman Shabani[1], Fatemeh Atyabi[2], and Masoud Soleimani[3]*

Young Researchers and Elites Club, Science and Research Branch, Islamic Azad University, Tehran 1477893855, Iran
[1]*Department of Biomedical Engineering, Amirkabir University of Technology, Tehran 15875-4413, Iran*
[2]*Nanotechnology Research Centre, Faculty of Pharmacy, Tehran University of Medical Sciences, Tehran 14155-6451, Iran*
[3]*Department of Hematology, Faculty of Medical Science, Tarbiat Modares University, Tehran 14115-111, Iran*
(Received December 20, 2014; Accepted January 13, 2015)

Abstract: In this study, nanofibers of poly(lactic-*co*-glycolic acid) with a core-shell structure encapsulating epidermal growth factor (EGF) were prepared through emulsion electrospinning technique. The morphology and the core-shell structure of the nanofibers were observed by field emission scanning electron microscopy and transmission electron microscopy, respectively. The release profile of EGF indicated a continuous release of the protein over one week. Biocompatibility of the plasma-treated scaffolds was evaluated using MTT assay for human fibroblast cells. The results demonstrated desirable biocompatibility and bioactivity of the scaffolds with the capability of encapsulation and controlled release of EGF which can be utilized in skin tissue engineering applications.

Keywords: Emulsion electrospinning, Nanofibrous scaffolds, Epidermal growth factor, Skin tissue engineering, Poly(lactic-co-glycolic acid)

Introduction

Providing a temporal support for the cells and controlling their behavior necessitates the utilization of scaffold systems in tissue engineering. An ideal scaffold affords to mimic the extracellular matrix (ECM) structure identically. The electrospun scaffolds possess high specific surface area, high porosity and interconnected pore network, which are architecturally similar to the natural ECM [1-6]. In addition to imitating the topography and composition of the ECM, the scaffold systems are also necessary to be integrated with macromolecular bioactive agents in order to regulate the cellular processes such as migration, proliferation and differentiation [7,8].

Tissue recovery after an injury is one of the natural processes involving several stages namely inflammation, cell proliferation and tissue regeneration. There are a number of cells and factors that influence the wound healing process and accelerate the tissue recovery. Amidst these, growth factors (GFs) which control wound healing events, are one of the most important elements. They are responsible for transmitting required signals to control cell proliferation, differentiation and ECM secretion. Topical gels containing GFs have been applied around the lesions however, this approach has not been very successful due to the quick diffusion and drying of the GFs in the lesion area [8,9].

Epidermal growth factor (EGF) has been one of the most prevalent factor for treating wounds. This is a polypeptide consisting of 53 amino acids which improves cell motility and proliferation as well as epidermal and mesenchymal regeneration. It has been proved that EGF possesses high-affinity receptors expressed in both fibroblasts and keratinocytes and is capable of accelerating wound healing [8].

Topically applying these molecules with a controlled release profile through a suitable wound dressing provides an efficient local concentration of EGF, protects it against *in vivo* degradation and protects the lesion during the healing process [8,10].

Several studies have employed using nanofibrous scaffolds as delivery systems for GFs. Choi *et al.* [11] conjugated EGF on the surface of electrospun poly (ε-caprolactone) nanofibers functionalized with amine groups via polyethylene glycol (PEG) linkers. In their study, the EGF-nanofibers facilitated wound healing processes *in vivo* significantly compared to the direct application of EGF solutions. In another study, Schneider *et al.* [10] demonstrated that bioactive EGF was released from electrospun silk nanofibers prepared by blend electrospinning. Yang *et al.* [9] also reported that basic fibroblast growth factor (bFGF) was encapsulated into ultrafine fibers. The bFGF loaded scaffolds were efficient in wound healing and skin regeneration.

Poly (lactic-*co*-glycolic acid) (PLGA) is a biocompatible and biodegradable polymer which possesses appropriate mechanical properties. It's utilization in drug distribution systems and a number of other clinical uses has been approved by the United States Food and Drug Administration (FDA) [12]. The application of PLGA nanofibrous scaffolds for the purpose of skin tissue engineering has been reported by Blackwood *et al.* [13] and Kumbart *et al.* [14].

The aim of this study was to prepare and evaluate poly (lactic-*co*-glycolic acid) (PLGA) electrospun nanofibers containing EGF with the capability of controlled release of the protein.

Experimental

Materials

PLGA (Purasorb®, PLG8523) was purchased from Purac, The Netherlands. Chloroform, acetone, bovine serum albumin

*Corresponding author: soleim_m@modares.ac.ir

(BSA), dimethyl sulfoxide (DMSO) and span 80 were all purchased from Merck, Germany. Dulbecco's modified Eagle's medium (DMEM), fetal bovine serum (FBS), phosphate buffered saline (PBS), trypsin, streptomycin and amphotericin were acquired from Gibco, USA. Recombinant human epidermal growth factor was supplied from PeproTech and Enzyme-linked immunosorbent assay (ELISA, Quantikine®) kit for EGF was purchased from R&D Systems, USA. MTT (3[4,5-dimethylthiazol-2-yl]-2,5-diphenyltetrazolium bromide) reagent and penicillin were obtained from Sigma-Aldrich, USA.

Preparation of Electrospun Nanofibers

The PLGA solution with a polymer concentration of 4.5 wt% in a mixed solvent system of chloroform/acetone in a 2/1 volume ratio was prepared. While chloroform is individually a suitable solvent for PLGA [12], the mixed solvent system of chloroform and acetone improves the electrospinning process due to the high dielectric constant of acetone. To prepare water-in-oil (W/O) emulsion, span 80 (Sorbitan Monooleate) in a 5 wt% ratio to the polymer weight was added into the polymer solution and afterwards, EGF solution with a concentration of 0.1 wt% (with respect to PLGA mass) in phosphate buffer saline (PBS, 50 mM, pH 7.4, BSA 1 wt%) as the aqueous phase was added dropwise into the polymer solution under stirring at 1000 rpm. BSA can act as a protector of the growth factor [15] and span 80 is utilized as a non-ionic and non-toxic surfactant in order to stabilize the emulsion [16].

The electrospinning system comprises several constituents including a power supply of high voltage, a polymer solution reservoir, a digital syringe pump and a conductive collection device. To overcome the liquid surface tension and enable the formation of polymer jet, a positive voltage of 16 kV was applied. The electrospun nanofibers were collected on aluminum foil covering the cylindrical collector located 10 cm away from the tip of the syringe needle with a rotation speed of 100 rpm. The electrospinning solution was flowing at a rate of 1 m*l*/h and the experiment was being administered at room temperature.

Plasma treatment is one of the most efficient methods to increase hydrophilicity of the surfaces which leads to enhance cell attachment, expansion and proliferation on the surfaces [17,18]. Therefore, a plasma generator (Diener Electronics, Germany) was used. Pure oxygen was introduced into the reaction chamber with a pressure of 0.4 mbar and the glow discharge was set on ignition for 5 minutes.

Characterization of Electrospun Scaffolds

The morphology of the scaffolds was observed using field emission scanning electron microscope (FESEM, Hitachi, S4160, Japan) with an accelerating voltage of 15 kV. For this purpose, specimens were sputter coated with gold prior to observation. Average diameter of the fibers was measured by Image-J analysis software (National Institute of Health, USA). Porosity of the scaffolds was calculated according to the equations (1), (2);

$$\rho a = \frac{m}{\pi r^2 h} \tag{1}$$

$$\varepsilon = \left(1 - \frac{\rho a}{\rho b}\right) \times 100\% \tag{2}$$

where m, r, and h are mass, radius and thickness of the electrospun nanofibrous mat, respectively [19]. Moreover, ρ_a and ε represent the apparent density and porosity of the mats. Bulk density (ρ_b) of PLGA was 1.29 g/cm^3 [19]. The core-shell structure of the emulsion electrospun PLGA/EGF composite nanofibers was examined by transmission electron microscope (TEM, Zeiss, EMLOC, Germany) with an accelerating voltage of 80 kV. Tensile characteristics of the scaffolds were measured by means of an Instron universal testing machine (STM-20, Santam Company, Iran). The samples with dimensions of length×width=50 mm×10 mm were prepared and elongated at a rate of 10 mm/min and the stress-strain curves were plotted. The tests were performed in triplicate.

In vitro Protein Release Study

In order to evaluate the amount of EGF released, the scaffolds with 10±1 mg weight were immersed into 1 m*l* of PBS containing 1 % penicillin/streptomycin and 1 % amphotericin as biocides and were incubated at 37 °C. At predetermined intervals, 100 μl of the medium was retrieved and an equal volume of fresh medium was replaced. Concentration of the EGF was determined using ELISA kit, specific for human EGF, according to the manufacturer's instruction.

Cell Isolation and Culture

Postnatal human foreskin tissue was provided from Sarem hospital considering the bioethics regarding the ownership and uses of human tissue. In order to isolate the fibroblast cells, the tissue was washed with PBS, treated with 0.5 % dispase/PBS and incubated at 37 °C for 1 hour. Then, the epidermis layer was separated by gentle agitation. The dermis layer was cut to 3 mm pieces and they were suspended in PBS containing 0.5 % trypsin and incubated under shaking at 37 °C for 30 minutes. Consequently the suspension was centrifuged to collect and separate the dispersed cells from the undigested tissue and debris. Afterwards, the cells were cultured and expanded in DMEM supplemented with 10 % fetal bovine serum, penicillin-streptomycin and amphotericine. Subsequently, the cells at the second passage were seeded on the surface-treated and UV-sterilized scaffolds at a concentration of 10000 cells/cm^2. The cultured specimens were incubated at 37 °C with 5 % CO_2 and relative humidity of 95 %. The cell culture medium was replaced every 2 days.

MTT Assay

The MTT colorimetric assay was employed to evaluate the cell viability and proliferation. The fundamental of the MTT assay is based on the appraisal of the cellular metabolic activities while blue crystals of formazone are being formed through the cleavage of tetrazolium ring of MTT. For this purpose, at determined intervals (days 1, 3 and 5), 300 μl of MTT solution was added to each well and incubated for 3 hours. Afterwards, the solution was removed and each well was supplied with 1000 μl of DMSO in order to dissolve formazone crystals. The solutions were retrieved once they were shaken and their absorbance was recorded at 540 nm using ELISA Reader (BioTek, USA).

Cell Attachment and Morphology

The specimens were studied through FESEM after a 5-day period of culture to observe fibroblast attachment and morphology on the scaffolds. For this purpose, all the specimens were washed with PBS in order to eliminate non-adherent cells and were consequently fixed at room temperature by being immersed in 2.5 % glutaraldehyde solution for 3 hours and were dehydrated in a sequence of ethanol aqueous solutions with incremental concentrations ranging from 50 % up to 100 %. Finally, the samples were dried and prepared for FESEM observation. Also, for cell nuclear staining, the samples were fixed in 3.7 % paraformaldehyde solution and then stained with 4-6-diamidino-2-phenylindole (DAPI). Subsequently, the samples were visualized with a fluorescent microscope (Nikon Eclipse TE2000-S; USA) at 405 nm.

Results and Discussion

Characterization of Electrospun Fibers

The morphology of PLGA nanofibers and the composite nanofibers (PLGA/EGF) is illustrated in Figure 1. The electrospun mats were constructed of randomly oriented fibers with a smooth and non-beaded morphology. Average diameter of PLGA nanofibers (Figure 1(a), (c)) was 670± 214 nm, while it decreased to 402±102 nm (Figure 1(b), (d)) once the protein and span 80 were introduced into the solution. In fact, the polymer jet which includes extra charge density faces to more elongational forces leading to formation of finer fibers. Also, the histograms in Figure 2 depict the diameter distribution of the nanofibers. The porosity of the scaffolds was obtained 88±2 % implying high porous scaffolds.

In TEM image (Figure 3(b)), the dark phase implies the protein which has been encapsulated in the core of the nanofibers while Figure 3(a) shows pure PLGA nanofibers [20,21]. The development of this core-shell structure is attributable to the immiscible nature of the two phases, i.e. the organic and the aqueous phases and also the fast solidification process of the jet which does not allow a considerable mixing of the two fluids. In fact, the viscosity of outer layer of the jet increases faster than one of the inner layers because of the rapid evaporation of chloroform and acetone. As a result, based on the viscosity gradient, the droplets of the aqueous phase migrate to the core of the jet. The emulsion droplets which possess a spherical form, experience substantial elongation during the electrospinning and significantly

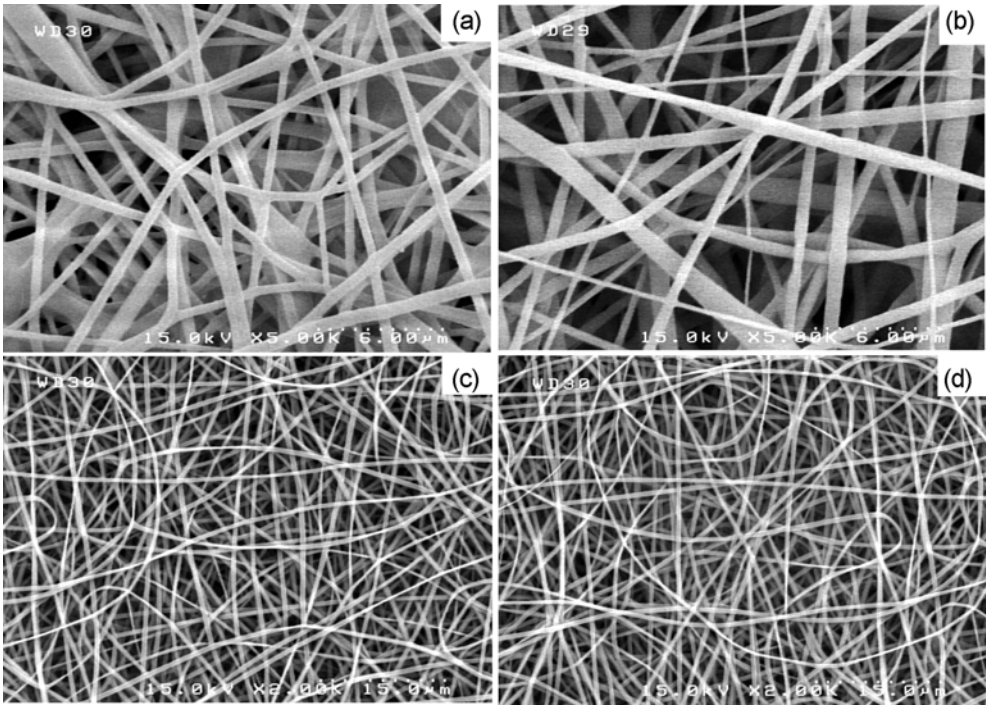

Figure 1. FESEM images of the nanofibrous scaffolds: (a), (c) PLGA and (b), (d) PLGA/EGF. 5000× and 2000× magnifications.

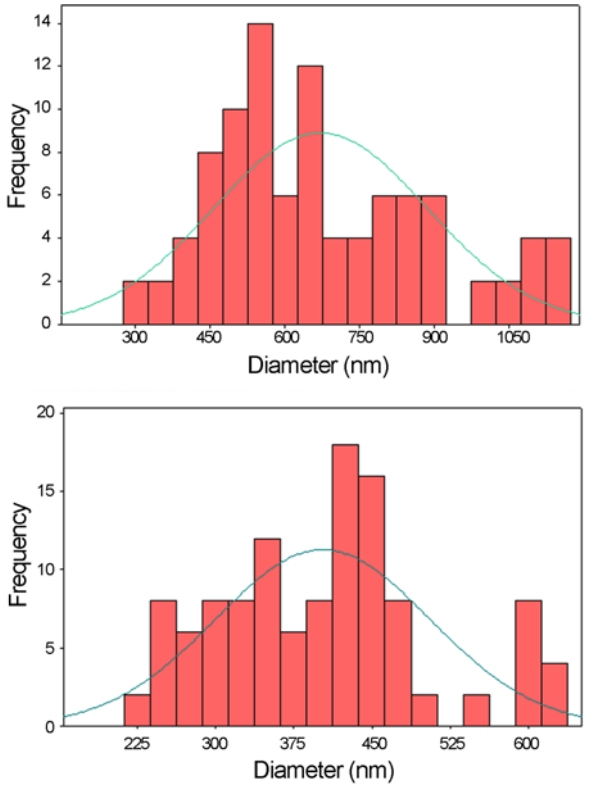

Figure 2. Histograms of the diameter distribution of the fibers; (a) PLGA and (b) PLGA/EGF.

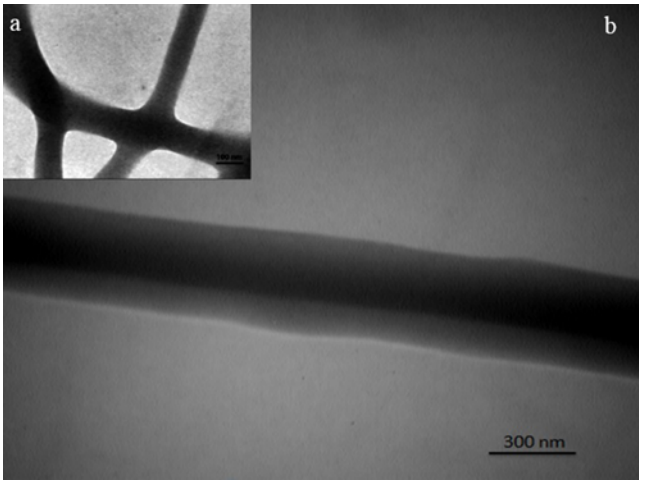

Figure 3. TEM images of (a) PLGA and (b) PLGA/EGF nanofibers.

lose their spherical layout while elongated [20,21].

Mechanical properties can be considered as one of the effective factors in the application of nanofibrous scaffolds in tissue engineering. Introducing protein to the nanofibers resulted in a decreased tensile strength. The ultimate tensile stress of PLGA and PLGA/EGF nanofibers were measured to be 1.3±0.2 and 0.8±0.2 MPa, respectively. This can be

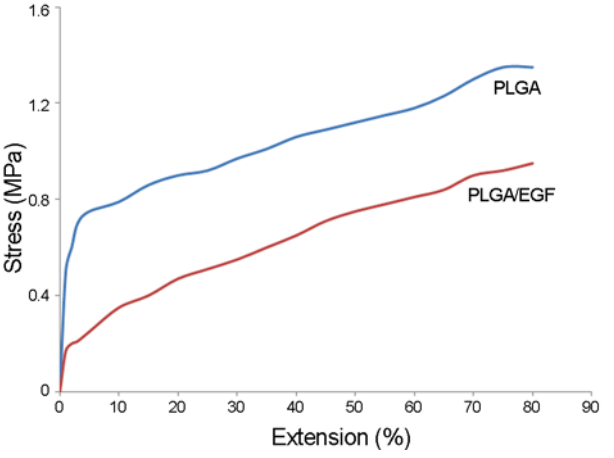

Figure 4. Representative tensile stress-strain curves of PLGA and PLGA/EGF nanofibers.

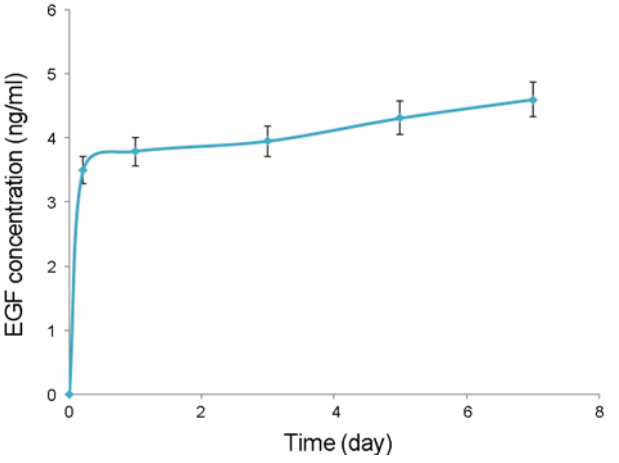

Figure 5. Release profile of EGF. The error bars represent one standard deviation from three replicate experiments.

associated with the formation of voids and cracks in the structure of the fibers resulted from the weak interfaces between the protein and the polymer (Figure 4).

In vitro Protein Release

Figure 5 illustrates the cumulative release of EGF from the composite nanofibrous scaffolds. The release profile comprises two stages: the burst release in the first day and the sustained release for the next days. The burst release can be explained by existence of a minor amount of the protein on the surface of the fibers or near it due to the incomplete inward movement of the emulsion droplets [22], while the sustained release is attributable to the protein in the core of the fibers. It was anticipated that the remaining encapsulated EGF would take longer to release. While, the gradient of EGF concentration declines between the core and the surface as EGF is released, the rate of EGF release decreases gradually. It is noteworthy that the release of drug generally takes two possible approaches

including diffusion according to the concentration gradient as mentioned above and also the polymer degradation which occurs in a longer period of time. It has also been suggested that the incorporation type of the protein considerably affects the release profile. Encapsulating the drug within core of the nanofiber leads to a sustained release while positioning it on the exterior of the nanofibers will cause a burst release at the beginning [23,24]. In this study, the effective released concentration of EGF in the 7th day was estimated 4.5±05 ng/m*l*.

The re-epithelialization of wound is a paramount process which is essential to begin with a considerable rate instantaneously after the occurrence of an injury in order to protect the body especially against microbes and water loss. Therefore, the burst release of EGF from the mat is crucial since it can activate the keratinocytes on the edge of the ulcer [9,10]. The burst release was obtained through the designed scaffold whereby the existence of protein on the exterior of the fiber. However, the next stage in the release profile incorporates a moderate escalation in which EGF molecules in the interior of the fiber diffuse to the surface of the fiber.

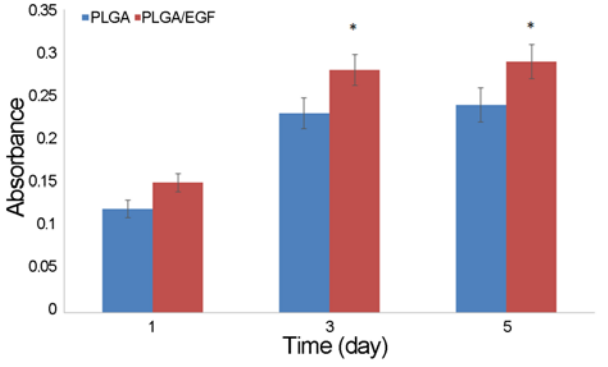

Figure 6. MTT assay of fibroblasts. The error bars represent one standard deviation from three replicate experiments. Asterisks show significant differences with $p<0.05$.

Throm *et al*. [24] reported the relation between optimal EGF concentration and the matrix strength as well as thickness. They declared that 0.5-5.0 ng/m*l* of EGF can effectively promote formation of a strong extracellular matrix in 3 weeks. In their study, the amount of 5 ng/m*l* of EGF was opted to increase the thickness of the matrix as much as possible although it may not have the same effects on collagen production.

Cell Attachment and Metabolic Activity

To measure the viability and proliferation of the cells, MTT assay was employed. In this regard, composite scaffold containing EGF proved advantageous to PLGA scaffolds in which it demonstrated superior bioactivity in terms of cell proliferation. In fact, the scaffold of PLGA/EGF which released the GF in a sustainable manner, improved the

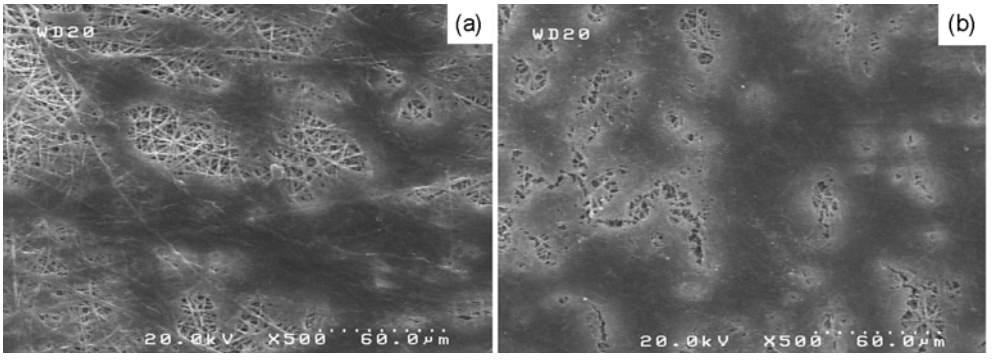

Figure 7. FESEM images of cell morphology on (a) PLGA and (b) PLGA/EGF nanofibrous scaffolds. 1000× magnification.

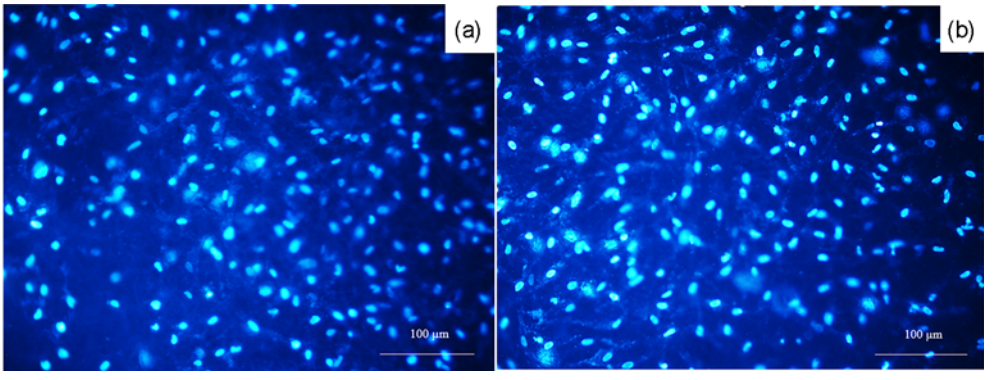

Figure 8. Fluorescence microscopy images of cells on (a) PLGA and (b) PLGA/EGF nanofibrous scaffolds. 40× magnification.

cellular proliferation (Figure 6). This is in correspondence with other studies that EGF can increase cell growth [8,11]. However, it seems that a confluence was reached on the 5th day. These results show the possibility of using bioactive agents to promote the cellular proliferation on the scaffolds.

Furthermore, the cell morphology observations revealed flattering and polygonal extensions of fibroblasts on both scaffolds of PLGA and PLGA/EGF (Figure 7). These results indicated the superior interaction between the cells and the nanofibers. Also, the fluorescence microscopy images of the stained cells are depicted in Figure 8 which imply the desirable cell distribution on the scaffolds.

Conclusion

Nanofibers of PLGA encapsulating EGF were fabricated through emulsion electrospinning technique. The average diameters of the PLGA and composite nanofibers were determined to be 670 nm and 402 nm, respectively. The core-shell structure of the EGF-loaded nanofibers was confirmed by TEM. Tensile characteristics of the scaffold demonstrated a reduction in the tensile strength of the composite nanofibers in comparison to PLGA nanofibers. The release profile of EGF illustrated a continuous release behavior of the protein within 7 days. Also, the MTT results of human fibroblast indicated desirable biocompatibility and bioactivity of the scaffolds. In general, preparation of the highly porous biocompatible scaffold with the capability of encapsulation and controlled release of the growth factor indicates its perspective applications in skin tissue engineering.

Acknowledgments

This work was financially supported by Stem Cell Technology Research Center (Tehran, Iran).

References

1. M. Norouzi, S. M. Boroujeni, N. Omidvarkordshouli, and M. Soleimani, *Adv. Healthc Mater.*, DOI: 10.1002/adhm.201500001, 2015.
2. Y. Yang, G. Tang, H. Zhang, Y. Zhao, X. Yuan, M. Wang, and X. Yuan, *J. Biomed. Mater. Res. Part B*, **96**, 139 (2011).
3. F. Zamani, M. Latifi, M. Amani-Tehran, and M. A. Shokrgozar, *Fiber. Polym.*, **14**, 698 (2013).
4. G. Panthi, N. A. Barakat, P. Risal, A. Yousef, B. Pant, A. R. Unnithan, and H. Y. Kim, *Fiber. Polym.*, **14**, 718 (2013).
5. M. A. Kanjwal, F. A. Sheikh, R. Nirmala, J. Macossay, and H. Y. Kim, *Fiber. Polym.*, **12**, 50 (2011).
6. F. A. Sheikh, N. A. Barakat, M. A. Kanjwal, A. A. Chaudhari, I. H. Jung, J. H. Lee, and H. Y. Kim, *Macromol. Res.*, **17**, 688 (2009).
7. D. Meng, M. Erol, and A. R. Boccaccini, *Adv. Eng. Mater.*, **12**, B467 (2010).
8. J. K. Choi, J.-H. Jang, W.-H. Jang, J. Kim, I.-H. Bae, J. Bae, Y.-H. Park, B. J. Kim, K.-M. Lim, and J. W. Park, *Biomaterials*, **33**, 8579 (2012).
9. Y. Yang, T. Xia, W. Zhi, L. Wei, J. Weng, C. Zhang, and X. Li, *Biomaterials*, **32**, 4243 (2011).
10. A. Schneider, X. Wang, D. Kaplan, J. Garlick, and C. Egles, *Acta Biomater.*, **5**, 2570 (2009).
11. J. S. Choi, K. W. Leong, and H. S. Yoo, *Biomaterials*, **29**, 587 (2008).
12. Y. You, S. J. Lee, B. M. Min, and W. H. Park, *J. Appl. Polym. Sci.*, **99**, 1214 (2006).
13. K. A. Blackwood, R. McKean, I. Canton, C. O. Freeman, K. L. Franklin, D. Cole, I. Brook, P. Farthing, S. Rimmer, J. W. Haycock, A. J. Ryan, and S. MacNeil, *Biomaterials*, **29**, 3091 (2008).
14. S. G. Kumbar, S. P. Nukavarapu, R. James, L. S. Nair, and C. T. Laurencin, *Biomaterials*, **29**, 4100 (2008).
15. C. M. Valmikinathan, S. Defroda, and X. Yu, *Biomacromolecules*, **10**, 1084 (2009).
16. K. Wei, Y. Li, X. Lei, H. Yang, A. Teramoto, J. Yao, K. Abe, and F. K. Ko, *Macromol. Biosci.*, **11**, 1526 (2011).
17. A. R. Chandrasekaran, J. Venugopal, S. Sundarrajan, and S. Ramakrishna, *Biomed. Mater.*, **6**, 015001 (2011).
18. G. H. Ryu, W. S. Yang, H. W. Roh, I. S. Lee, J. K. Kim, G. H. Lee, D. H. Lee, B. J. Park, M. S. Lee, and J. C. Park, *Surf. Coat. Technol.*, **193**, 60 (2005).
19. A. G. Mikos, G. Sarakinos, S. M. Leite, J. P. Vacant, and R. Langer, *Biomaterials*, **14**, 323 (1993).
20. M. Norouzi, M. Soleimani, I. Shabani, F. Atyabi, H. H. Ahvaz, and A. Rashidi, *Polym. Int.*, **62**, 1250 (2013).
21. M. Norouzi, I. Shabani, H.H. Ahvaz, and M. Soleimani, *J. Biomed. Mater. Res. A*, DOI: 10.1002/jbm.a.35355, 2014.
22. Y. Yang, X. Li, W. Cui, S. Zhou, R. Tan, and C. Wang, *J. Biomed. Mater. Res. A,* **86**, 374 (2008).
23. A. Szentivanyi, T. Chakradeo, H. Zernetsch, and B. Glasmacher, *Adv. Drug Deliv. Rev.*, **63**, 209 (2011).
24. A. M. Throm, W. C. Liu, C. H. Lock, and K. L. Billiar, *J. Biomed. Mater. Res. A*, **92**, 533 (2010).